

ANALYSIS OF CORRELATION BETWEEN THE EXPANSION RATE AND THE INDEX OF REACTIVITY DETERMINED BY PETROGRAPHY

E. Menéndez^{1*}, R. García-Rovés¹, N. Prendes², S. Ruíz³

¹Institute “Eduardo Torroja” of Construction Science (CSIC), Madrid, [SPAIN](#)

²CEDEX. [SPAIN](#)

³Dragados, S.A. [SPAIN](#)

Abstract

One of the most common methods to evaluate the potential reactivity of the aggregates is the accelerated mortar bar test that permits to qualify the reactivity at 14 or 28 days. The extension in the time of this test is showing the total potential expansion of the aggregates and the ratio of this expansion.

With the petrographic analysis it is possible to determine the tortuosity of the interface between reactive particles or of the pores in the aggregates. These are analyzed by digital image treatment and generate an index of reactivity. This index of reactivity is a function of the quantity of reactive particles and the tortuosity of the borders of reactive grains.

In this work the correlation between the expansion rate and the petrographic index of reactivity has been analyzed. The studied aggregates were used in different structures that have shown ASR after some years on environmental conditions.

Keywords: Potential reactivity, expansion rate, index of reactivity, petrography, aggregates

1 INTRODUCTION

Research into the behavior of some aggregates as construction materials, for some specific physical-chemical conditions of concretes, have demonstrated their reactivity against certain alkaline components, generating products or highly expansive phases which may occasionally bring about the collapse of their structures and a significant deterioration [1,2].

The most common reaction between alkalis and aggregates in concrete is the alkali-silica or alkali-silicate, in which a reaction between the poorly crystallized aggregates of a natural silica and the alkalis present in the concrete form silico-calco-alkaline hydrate gels of an expansive nature, takes place.

There have been numerous tests into the prediction of the behavior of the constituents of the concretes, related to the different types of internal expansive reactions. The objective of these tests is to analyze the different aspects of each of these phenomena, with the intention of deciding the convenience of using or not a certain constituent (aggregates, cements, additions, additives, etc.), however, the intention for this is to generate the specific event, using the factors that affect the different processes to accelerate their appearance.

From the identification of the damage, resulting from alterations brought about by the alkali-aggregate reaction, numerous test methods have been developed to qualify the components of the concrete (especially the aggregates), with the aim of predicting the appearance of this reaction. The most used test methods for the prediction of the alkali-aggregate reaction are based on the ASTM (American Standard of Testing Materials) regulations; even though some of them are based on Canadian or South African procedures.

The most currently used methods are the ASTM C1260 (Accelerated method of mortar bars), ASTM C1293 (Prism method of concrete), ASTM C227 (Semi-accelerated method of mortar bars), ASTM C295 (Petrographic analysis of the analysis of the aggregates) and ASTM C289 (Chemical method). Some of these regulations are based on other test methods, or have their counterparts in other ones.

* Correspondence to: emm@ietcc.csic.es

The paradigm makes up the quartz (SiO_2), which is the most abundant tectosilicate in siliceous rocks, and the most common aggregate in the concretes, whose behavior depends on its nature [3,4,5].

Quartz has a trigonal symmetry, and can become monoclinic and triclinic, according to the temperature and formation pressure, with a great variety of polymorphs and mixed aggregates, what, crystallographically means that its reticular mesh must absorb tensions which translate into reticular dislocations and defects or intercrystalline disorders which become apparent in the development of subgrains and structural stacking in the quartz specimen itself [6,7]. These phenomena give rise to manifestly reactive varieties such as opaques, chalcedonies, cristobalites and trydimites, which maintain the chemical configuration of the quartz [8].

Quartz has an opaque property called undulose extinction, when it is observed in a thin section using optical microscopy with polarised light. This property represents the degree of deformation of the crystalline network of each grain, generating internal areas with different orientations. The limits between the different areas of deformation are areas with a high level of dislocation. The degree of extinction of the quartz is a function of the different formation processes of the rock in which the content is found [7]. The development of subgrains in the deformed quartz crystals will contribute to a greater reactivity due to the high density of dislocation associated with the subgranular limits [9].

The extinction edges are open areas with chains of Si^{2+} -type radicals capable of fixing groups of high labile OH- siloxane through alkaline or alkaline earth metal cations, favouring the development of very reactive products [10], which are the base or nucleation of the expansive gels in a later stage.

The petrographic studies and analysis with different species of SiO_2 that relate the reactivity of the quartz with the reticular state have been dealt with by different authors [11,2,12]. These studies were carried out from the qualitative point of view and only using optical microscopy, basing its measurements only on the undulate extinction angles of the quartz. Later, and by means of image processing techniques, this phenomenon is quantified in accordance with geometric and spatial parameters, such as the perimeters and areas of exposure, mapping the contacts, and establishing reactivity as a factor or index associated with this deformation [13,14,15,16].

The ASTM C1260 test method or its equivalents AASHTO T 303, CSA A23.2-25A and RILEM TC 106-2, (Accelerated method of mortar bars) is perhaps the most used of the accelerated test methods. It is often modified to evaluate specific mixtures of aggregates for its use in the manufacture of certain concretes.

The ASTM C1260 test is an accelerated method of mortar bars, which may be regarded as conservative in the sense that it provides an excess of alkalis (NaOH 1N) in the solution in which the test samples remain immersed and at a high temperature (80°C). The limitation is that in reality there is no external source of alkalis which corresponds to NaOH. However, this test isn't always useful for the identification of aggregates that react slowly and that cannot be evaluated by any other method. And, in general, it is hoped that the aggregates that are qualified as innocuous have a good functioning in the concrete. In accordance with this test method, the maximum expansion accepted in the United States for the aggregate to be considered as inoffensive is 0.1% [17] (14 days after a reading of zero or 16 days after its manufacture), or 0.15% in Canada (in accordance with the CSA A23.2-25A regulation, although 0.1% is recommended in Appendix B of the CSA A23.1) document [18,19]. However, these limits have been reduced to 0.08% in the case of metamorphic aggregates. Likewise, in Note X1.1 of the ASTM C 1260 it is indicated that some granite gneisses and metabasalts have turned out to be expansive in use, with an expansion of less than 0.1% after 16 days from manufacture. Also, in relation to the test limit, the ACI 221.1R (1998) document advises a limit of 0.08% to be used [20], just like Grosbois and Fontaine (2000) who suggest a limit of 0.08% or even 0.06% [21].

In this test it is proposed that the solution provides a sufficient external source of alkalis to complete any reaction and that the alkali content of the cement has no, or little, influence. However, different results have been observed using different types of cement when they have additions. In these cases it is recommended to use the maximum expansion limit of 0.1%.

We are trying to analyze the relationship between the reactivity analyzed at the petrographic level and the potential expansion obtained in the accelerated expansion test. To do this, four granite aggregates and one limestone aggregate have been collected and analyzed petrographically, the reactivity of the quartz content has been measured and an accelerated expansion test has been carried out.

2 MATERIALS AND METHODS

2.1 Materials

Four granite aggregates and one limestone aggregate were selected for this study. Two of them were used in concretes for dams, which have demonstrated damage over time due to the alkali-

aggregate reaction, and the other three aggregates from quarries are also destined for their use in the manufacture of concretes for dams.

The different aggregates tested are detailed in Table 1, specifying the origin and petrographic classification in accordance with the ASTM C294 regulation [22]:

2.2 Methods for assessment and analysis

General

The test methodology is established at two levels: The petrography of the aggregates and the accelerated expansion of the mortar bars. The test methods are described below.

Petrography by means of optical microscopy

Petrography of a representative sample of aggregate which is analyzed by means of a fine section using Olympus BX51 equipment. The mineralogy and composition is deduced.

The petrographic classification is carried out in accordance with the ASTM C294 regulation, which presents a more detailed classification than that set out in the UNE-EN 932-3 Regulation [23].

The optical response of each crystal is also visualized, discovering its reticular structure and with it, its tensional state, limiting the areas of the reticular mesh with the same crystallographic orientation.

The reactivity index of the quartz is calculated using image processing techniques, associated with their deformation, and the percentage of existing reactive quartz is estimated.

It could be argued that this index gives a spatial relationship of capacity contribution of siloxane groups to the interstitial solution, since it is accepted that the phases are reactive from the contact areas (structures which are porous or have fissures, capable of connecting different points between constituents) marking the relationship between edge contacts (percentage of phases that share common borders).

The following mathematical equation is used to determine the reactivity index [13,14,15,16]:

$$I_{Qr} = \frac{P_{ext}}{P_{ext} + P_{int}}$$

Where:

I_{Qr} = Reactivity index of the quartz (dimensionless)

P_{ext} = Perimeter of the exterior edge of the grain

P_{int} = Internal perimeters with individualized phases of undulate extinction

If the reactivity index tends towards 1, it is a more stable and ordered crystallographic network, though $1 < I_{Qr} < 0.7$ indicate stable structures and without defects, and $0.7 < I_{Qr} < 0.4$ indicate structures with some defects, but stable. If this index approximates to 0, it is a consequence of a high deformation and reticular asymmetry and $0.4 < I_{Qr} < 0$ indicate deformed and fractured structures, developing phases with undulose extinction. A value very close to zero is mathematically impossible to obtain due to a purely geometrical problem and limits in reticular deformation.

The experimental data correlated with quantitative values, fixes a threshold to define the potential reactivity of $I_{Qr} = 0.38$ [12] or $I_{Qr} = 0.25$ [24]. Below these values it is considered that the quartz it potentially reactive.

As a complementary petrographic analysis, it also carries out a classification of the aggregates in accordance with the recommended RILEM AAR-1 test method [25]. This method consists of a general procedure for the petrographic examination in concretes, useful in identifying the types of rocks and minerals which may react with the hydroxyl ions of the interstitial solution of the concrete.

The main objective of the method consists of classifying an aggregate in terms of alkaline reactivity, through the presence of potentially reactive mineralogical phases, which favor reactivity.

As a result of subjecting an aggregate to the RILEM petrographic examination, this would be classified qualitatively in one of the following classes:

- Type I – Improbable reactivity with alkalis
- Type II – Inconstant reactivity with alkalis. The aggregate cannot be classified definitively in classes I and III
- Type III – Very probable reactivity with alkalis

This method demands previous geological, petrographic and tensional knowledge of the aggregate together with its behavior in similar uses. In this study, the points counter is substituted by

digital image processing techniques, assigning it the corresponding identifier of the Table 2 which is perfectly correlated with the classification of the ASTM C-294.

Expansion according to the ASTM C1260 regulation

This method is based on the measurement of the change in length experienced by a series of mortar samples made with the aggregate that we want to study, after having been submerged in water at $80^{\circ}\text{C} \pm 2^{\circ}\text{C}$ for the first day and a solution of NaOH 1N at $80^{\circ}\text{C} \pm 2^{\circ}\text{C}$ for the 14 following days.

Depending on the expansion obtained in the samples, at 14 days of alkaline treatment, the following classification may be made:

- If the expansion is less than 0.10%, the aggregate may be considered as non-reactive.
- If the expansion is more than 0.20%, the aggregate may be considered as potentially reactive.
- If the expansion is between 0.10% and 0.20%, length measurements are taken from the samples up to 28 days.
- If after 28 days the expansion remains between 0.10% and 0.20%, it is necessary to obtain complementary information to be able to classify the aggregate. For this, together with the petrographic examination and other tests to evaluate its reactivity, an examination of the samples may be carried out after the test to identify the products of the reaction by means of electronic microscopy techniques.

3 RESULTS

3.1 Petrography by means of optical microscopy

The following results are obtained from the petrographic analysis carried out on the studied aggregates, by means of optical microscopy:

The CL sample:

The main phases are calcite, in the form of micrites and sparites, and dolomite in very limited sequences. Siliceous compounds are also observed, highlighted among which are quartz, generally stable, with straight extinction and relatively small sizes of less than $0.4\ \mu\text{m}$, including nodules and partial recrystallizations in the form of microcrystalline quartz. Calcium feldspar, potassium feldspar, and phyllosilicates are also identified from the group of biotite- and muscovite-type micas. Chlorites and illites are also identified, stable and as secondary alteration processes. As accidental mineralogical phases, pyrites, marcasites, and complex carbonates are observed such as ankerites or siderite, or secondary sulphates of glauconite-type alteration.

The GS sample:

Feldspars, quartz and micas are mainly observed, with an equigranular texture, with an average-sized grain. The aggregate presents a certain degree of cracking. Idiomorphic quartz crystals and some microgranular aliotriomorphic crystals are observed. The presence of quartz with undulose extinction is observed, some with saturated edges and mirrequisitisation processes. Other smaller-sized quartz is detected, which present sarcoid sandstone structures, which locally makes them increase their undulose extinction and therefore, increase their possibility of being reactive.

The detected feldspars are of the potassium feldspar and plagioclase in very similar proportions. The plagioclases are mainly of the albite-oligoclase type, that is, they are a very sodium-rich plagioclase and, therefore, relatively stable. The presence of antiperite is fairly frequent and the host mineral is totally sericitized. Illites and chlorites have also been found.

The potassium feldspars are much more altered than the plagioclase, presenting zoning and deformations of a mechanical type, with deformations and fissures in the crystals, certainly associated with selective flows in the magmatic segregation. For this reason sericites are produced which are visible in the antiperites. The presence of chlorites and illites is greater in the altered area than in the areas with no alteration.

The phyllosilicates from the group of micas are mainly biotite and muscovite, some of which have a certain degree of alteration. As accidental mineralogical phases, apatite, zircon halos and opaques such as pyrite or chalcopyrite, generally present in the phyllosilicates have been detected. Very altered hornblendes are occasionally detected, which could lead to the liberation of cations of iron and magnesium. Chlorites coming mainly from the alteration of the muscovite and some biotites have also been detected.

The GE sample:

Quartz, feldspars and micas have appeared as essential mineralogy. This rock presents an inequigranular texture, heterogeneous in grain size, with idiomorphic to sub-idiomorphic quartz crystals. The most frequently found particles are between 200 μm and 1 mm in size.

Quartz with upright extinction and undulose extinction phases are observed. The feldspars are altered, with very well differentiated areas and deformations of a mechanical type, such as the fissures in the crystals. Sericites originating from an alteration in the feldspars are detected. Biotite and muscovite-type micas are also observed, with a laminate-like aspect and brown colorations, which are due to the pleochroism that they have. The phyllosilicate phases are sometimes associated with some opaque minerals such as pyrites and chalcopyrites and areas of alteration such as zircon halos and rutile, generally contained in the biotite. Some pertites and chlorites are also appreciated. The chlorites are more associated to the alteration of the muscovite.

The GB sample:

The main mineralogical phases are feldspars, quartz, and micas. The average size of the grains of feldspar and quartz are between 0.13 mm and 0.22 mm. In general, when comparing the sizes of these mineralogical phases, the feldspars are more developed, with orientated phenocrystals and of a larger average size.

Alkaline potassium feldspars of the microcline type have been identified in the feldspars, characteristic of its systems of intersecting in bars, and plagioclase as albites and oligoclases, with polysynthetic intersections, in extinction planes parallel to each other.

Associated to the mineralogical phases of the feldspars appear the mica-type phyllosilicates, both of a biotite- and muscovite-type. The percentage of mica is relatively low with respect to the other phases present in the aggregate. The alteration of the phyllosilicates is to secondary minerals, chlorites and sericites, which are very irregular in shape and with an acicular aspect.

The GG sample:

The predominant minerals are feldspars and quartz. Here crystals of feldspars and micas are segregated in a continuous series, evidencing the slow cooling temperature of the magma. Pertites and antipertites are also observed. The average size of the grains of feldspar and quartz is very similar, around 0.15 mm. Even though the feldspars, on being better developed and growing with a regular prismatic habit, sometimes give greater grain sizes in their crystals against those of the quartz, which are almost a third lower, even though they tend towards equigranularity.

There are two types of feldspar: alkaline and plagioclase, with the latter predominating. They are very altered, deformed and with selective areas according to the anortite content of the phase. The feldspars maintain their sub-idiomorphic habit, although partially blurred due to the alteration process.

The quartz evidences both undulose and upright extinction phenomena.

Biotite- and muscovite-type micas are observed. Some opaque minerals, such as pyrites and chalcopyrites and areas of alteration through pleochroic halos of zircon and rutile, are found associated to these phyllosilicate phases.

Quantitative analysis was carried out on the thin sections by means of the use of digital image processing and the percentages of the main mineral phases were quantified as detailed in Table 2.

Introducing the recalculated percentages of the mineralogical phases, quartz, potassium feldspar and plagioclase, of the GS, GE, GB and GG samples in the upper ternary Streckeisen diagram for the classification of igneous rocks [26], these aggregates were classified in the fields of granite and Granodiorites, as can be seen in Figure 1, that also corresponds to the classification given in the ASTM C294 and UNE-EN 932-3 regulations.

Using the simplified Classification diagram of sedimentary rocks from (Vatan, 1967) [27], the CL sample is classified as sandy limestone, as can be seen in Figure 2.

Although the granite aggregates have a similar mineralogical behavior (Figure 1 (a)), the plagioclase feldspars and ortoclases are partially altered to sericites and chlorites, favouring the alkaline solution with tardy reactivations during the hardening stages of the concrete, even though the albite-anortite plagioclases are more stable.

The biotite and muscovite micas have almost the same alteration behavior, supplying Al^{3+} , Mg^{2+} , Fe^{2+} and Fe^{3+} ions. The opaque minerals (chalcopyrite, pyrite, marcasite, pyrrhotite, etc.) mainly present in the GS and CL samples, supply sulphur ions that derive in (SO_4^{2-}) and those in sulphoaluminates in extremely alkaline environments.

The difference between the four granite aggregates is in the reticular structure of the quartz. Table 3, summarises the percentages of the tensionally deformed phases (saturated edges, sugary sandstone, microgranular textures, local defects, undulose extinction and microfissuring of the

transgranular type) drawn up from a representative number of specimens, and considering its structure through optical microscopy.

Quartz susceptible to reacting with the alkalis oscillated between 85% (GS) and 50% (GE) and it is shown at Table 3. The reactivity threshold I_{Qr} is fixed for all those aggregates which have $I_{Qr} < 0.3$. However, and in spite of the lower apparent percentage from this deformed phase of the GB and GG aggregates, these give a more reactive I_{Qr} and, therefore, a greater capacity for fixing the expansive gels in the final phases of more than 120 days.

This idea, based conceptually on the relationship between the deformational state of the quartz crystals and expansive gels have been contemplated by (Sims, I. Hunt, B. & Miglio, B. 1990) [2], associated with different ambient circumstances, from petrography and, in the long term, taking the table of (Mather, K. 1966) [1] as a reference that, for the first time, takes the crystallographic state more into account than the percentage of each mineral species.

From the results it was confirmed that the GG and GB mortars, with lower total percentages of deformed quartz, were not so reactive and susceptible, as they does not have a sufficient exposed surface per open edge [12] in which it would be fixed, due to the liberation of the siloxane groups in the interstitial solutions, in the expansive products [11] retarding the appearance of the ceolitical-type structures (gels). Evidently, this casuistry influences the redistribution of the porous system. The evolution of this process during the texturing of the concrete is the cause of the different behavior of these granite aggregates as potentially reactive [12], both for the fast and slow effect.

From the quantification of the mineralogical phases present in Table 2, the recommended method of RILEM AAR-1, classifies the analyzed aggregates in the classes as detailed in Table 4.

Expansion in accordance with the ASTM C1260 Regulation

From the accelerated test on bars of mortar ASTM C1260, only the GS aggregate were potentially expansive at 14 days (Figure 3). The rest of the aggregates were classified as non-reactive. At 28 days the GE and CL aggregates were plotted above the threshold of 0.1% of expansion.

The tests were prolonged over time so as to observe their evolution, obtaining very similar expansion values at 1 year (Table 5).

It was observed that all of the aggregates studies were expansive in the long term (Figure 4). The GS, GE, GB, GG granite aggregates were the ones that presented the greatest expansion value in the long term, taking an approximated asymptotic value of 0.70% of expansion.

On the other hand, alkali-aggregate reaction products were found, complex silico-calco-alkaline gel-types in all of the mortars, what indicates that, as well as the hydration of the mixture, other physical-chemical mechanisms intervened linked to certain specific mineralogical properties of the aggregates such as tensional, crystal-chemical state, or porosity. This would guarantee the slow reaction processes.

Several intervals associated with the texturing and expansivity of the samples can be identified in Figure 5. A first interval in which rapid reactions of cationic fixing are generated was observed after forty days, linked to the incipient hydration processes at high speeds in the texturing kinetics, favouring the development of new reticular phases, and epitaxial growth is associated to remaining solutions in the porous network. That which an aggregate has in this first interval with significant increases of expansion, is associated to a high reactive capacity, accepting that this will continue producing in the long term, as affirmed in the mortar of the GS aggregate.

From forty days there appears a second phase in which the texturing process of the mortars completes gradually. The saturated solutions are confined to areas of remaining porosity, and through chemical imbalance activating the alkaline coming from the aggregates which have been inert until now, as set out in Figure 5, in which there appear several peaks at different ages (120 days, 240 days, etc.), less significant, with specific increases which tend to mitigate over time.

4 CONCLUSIONS

The main difference between the aggregates analyzed, is in the reticular structure of the quartz. Within the grains of quartz considered as potentially reactive from the study of its reactivity index, the increase in subgrains and deformation flat generated during the deformation processes, increase the surfaces of the ionic exchange which consequently increases its potential reactivity. The greater the percentage of reactive quartz with respect to the total percentage of the quartz from each sample, the greater is both its potential reactivity and the percentage of expansion at the different ages.

All of the samples that contain reactive quartz have greater percentages of expansion when the test of the mortar bars is prolonged over time, reflecting this behavior in the asymptotic values of the percentage of expansion. Thus, even with the granite aggregates, that were classified as non-reactive

by the accelerated expansion tests, the expansion values continue to increase over time, indicating that these aggregates present a certain degree of long-term reactivity.

5 REFERENCES

- [1] Mather, K., 1966. Petrographic Examination of Hardened Concrete in Significance of Tests and Properties of Concrete-Making Materials. Symposium on Significance of Tests and Properties of Concrete and Concrete making Material. ASTM 169 A, Am.Soc. Testinf Mats, 1966, pp. 125-143.
- [2] Sims, I., Hunt, B. & Miglio B., 1990. Quantifying Microscopical Examinations of Concrete for Alkali Aggregate Reactions (AAR) and Other Durability Aspect, s.l.: ACI. pp. 267-287.
- [3] Dana J.D., 1863, Manual of geology. Theodore Bliss and Co.
- [4] Fernández Cánovas, M., 1996. Hormigón. 4º ed. Madrid. Colegio de Ingenieros de Caminos.
- [5] Bustillo Revuelta, M., Calvo Sorando, J.P., Fueyo Casado, L. 2001. Rocas industriales. Tipología, aplicaciones en la construcción y empresas del sector. Editorial rocas y minerales.
- [6] Broekmans, Maarten A.T.M., 2004. Structural properties of quartz and their potential role for ASR. *Materials Characterization* 53 (2004), pp129–140.
- [7] Smith, A.S., 1997. Quartz bearing aggregates and their role in the alkali-silica reaction in concrete prism tests, Thesis doctoral, University of Leicester.
- [8] Hobbs, D.W. 1988. "*Alkali-silica reaction in concrete*". Thomas Telford, London.
- [9] Wigum, B.J. 1995. Examination of microstructural features of Norwegian cataclastic rocks and their use for predicting alkali reactivity in concrete. *Engineering Geology* 40, pp. 195-214.
- [10] Glasser, F., 1992. Chemistry of the Alkali-Aggregate Reaction. In: Swamy, Ed. *The alkali-silica reaction in concrete*. Glasgow, pp. 2-28.
- [11] Dolar-Mantuani, L., 1981. Undulatory Extinction in Quartz used for Identifying Potentially Alkali-reactive Rocks. Cape Town, np, p. 11.
- [12] Grattan-Bellew, P. E., 1993. Is High Undulatory Extinction in Quartz Indicative of Alkali-Expansivity of Granitic Aggregates?.
- [13] Menéndez, E., Prendes, N., García-Rovés, R. 2015. Evaluation of potential reactivity of aggregates by the definition of the reaction index. Send to publish
- [14] Menéndez Méndez, E., García-Rovés Loza, R., Prendes Rubiera, N., Ruiz, S., 2015. Metodología avanzada de evaluación petrográfica de áridos para predecir su potencial reactividad frente a los álcalis del hormigón. IV Congreso Nacional de Áridos, Madrid.
- [15] Menéndez Méndez, E., Prendes Rubiera, N., García-Rovés Loza, R. 2014. Petrographic study of siliceous aggregates. Calculating parametric alkali reactivity. VII International PhD Student Workshop 2014, "service Life and Durability of Reinforced Concrete", IETcc-CSIC, Madrid
- [16] Menéndez Méndez, E., Prendes Rubiera, N., García-Rovés Loza, R. 2014. Estudio petrográfico de áridos silíceos. Cálculo paramétrico de su reactividad frente a los álcalis. Jornadas Internacionales Conmemorativas del 80 Aniversario del IETcc. IETcc-CSIC, Madrid
- [17] ASTM C1260. Standard test method for potential alkali reactivity of aggregates (mortar-bar method), American Society for Testing and Materials, Philadelphia, USA (1994)
- [18] CSA A23.2-25A, Test Method for Detection of Alkali Silica Reactive Aggregate by Accelerated Expansion of Mortar Bars, Canadian Standards Association, CSA International, Toronto, Ontario, CA, (2000)
- [19] CSA A23.1, Concrete Materials and Methods of Concrete Construction, Canadian Standards Association, CSA International, Toronto, Ontario, CA. 31, (2000)
- [20] ACI 221.1R-98. State-of-the-Art Report on Alkali-Aggregate Reactivity. American Concrete Institute.
- [21] Grosbois, M. de y Fontaine, E., 2000. Evaluation of the Potential Alkali Reactivity of Concrete Aggregates: Performance of Testing Methods and a Producer's Point of View, 11th International Conference on Alkali Aggregate Reaction, Québec City, Canada, pp. 267-276, (2000)
- [22] ASTM C294. Standard Descriptive Nomenclature for Constituents of Concrete Aggregates. ASTM Standards. Pennsylvania: ASTM Int.
- [23] UNE-EN 932-3. Ensayos para determinar las propiedades generales de los áridos. Parte 3: Procedimiento y terminología para la descripción petrográfica simplificada. Aenor.
- [24] Poole, A., 1992. Introduction to alkali-aggregate reaction in concrete. In: Swamy, ed. *The alkali-silica reaction in concrete*. pp. 2-28.

- [25] RILEM, 2003. AAR-1-Detection of potential alkali-reactivity of aggregates —Petrographic method, Materials and Structures 36, pp 480–496
- [26] Streckeisen, A. L., 1974. Classification and Nomenclature of Plutonic Rocks. Recommendations of the IUGS Subcommittee on the Systematics of Igneous Rocks. Geologische Rundschau. Internationale Zeitschrift für Geologie. Stuttgart. Vol.63, p. 773-785.
- [27] Vatan, V. M., 1967. Manual de sedimentología. Ed. Technip. Paris, 397 pp.

TABLE 1: Relationship of samples for test.

Sample code	Petrographic classification	Origin
CL	Sandy limestone	NE Iberian Peninsular
GS	Granite	NW Iberian Peninsular
GE	Granodiorite	NE Iberian Peninsular
GB	Granodiorite	NW Iberian Peninsular
GG	Granodiorite	NW Iberian Peninsular

TABLE 2: Mineralogical phases.

Sample code	Mineralogical phases								Petrographic Classification	
	Essentials (%)					Accessories (%)		Accident (%)		
	Calcite	Quartz	Potassic K-feldspar	Plagioclase	Micas	Moscovite	Chlorite	Opaque		
CL	60	30	10							Sandy limestone
GS	--	19.5	23.2	34.5	15.3	4	2.7	0.8	Granite	
GE	--	35	10	42	--	12	--	1	Granodiorite	
GB	--	27.8	20.8	41.4	10	--	--	--	Granodiorite	
GG	--	28	20.1	45.9	6	--	--	--	Granodiorite	

TABLE 3: Analysis of the reactivity of the quartz.

Sample	Q _{total} (%)	Q _{React} (%)	%Q _{reactive} of the %Q _{total}	I _{Qr} (Dimensionless)	Reticular state of the Q
CL	30	0	0	~0.89	Microgranular crystals with upright extinction
GS	19.5	16.1	82.5	~0.26	Microgranular crystals, fissured and saccharoidal
GE	35	21	60	~0.20	Branched fissuring, with saturated edges
GB	27	13	48.14	~0.09	Microfracturing and transgranular fissures
GG	28	15	53.57	~0.13	Microfracturing and transgranular fissures

TABLE 4: The classification of aggregates in accordance with RILEM AAR-1.

Sample code	Type	Potentially reactive mineralogical phases
CL	Type I	--
GS	Type III-S	Deformed quartz with a high reticular deformation, quartz sacaroid sandstone, feldspars Altered, micas and occasional opaques
GE	Type II-S	Deformed quartz, very altered micas and altered feldspars
GB	Type II-S	Deformed quartz and altered feldspars
GG	Type II-S	Deformed quartz and altered feldspars

TABLE 5: Expansion values.

Sample code	Expansion (%)			Mathematical adjustment	
	14 days	28 days	365 days	Function	R ²
CL	0.081	0.148	0.42	$y = 8E-09x^3 - 7E-06x^2 + 0.0023x + 0.064$	0.97
GS	0.104	0.200	0.69	$y = 3E-08x^3 - 2E-05x^2 + 0.0051x + 0.0711$	0.96
GE	0.062	0.127	0.66	$y = 1E-08x^3 - 9E-06x^2 + 0.0038x + 0.0207$	0.99
GB	0.048	0.081	0.62	$y = 5E-09x^3 - 6E-06x^2 + 0.0032x - 0.0021$	0.99
GG	0.055	0.084	0.65	$y = 3E-09x^3 - 5E-06x^2 + 0.003x + 0.004$	0.99

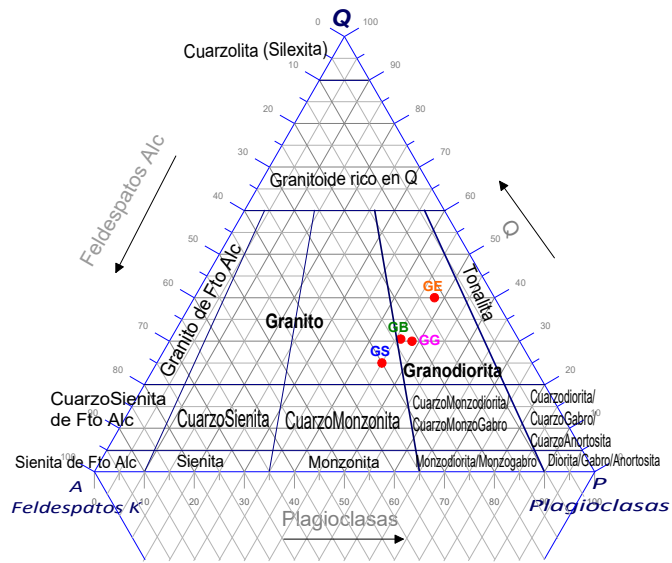


FIGURE 1: Classification diagram for igneous rocks (Streckeisen, 1974) [26].

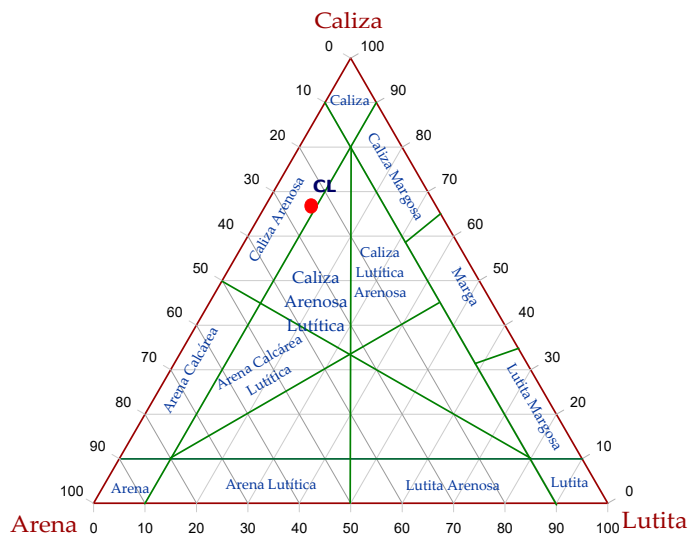


FIGURE 2: Simplified classification diagram for sedimentary rocks (Vatan, 1967) [27]

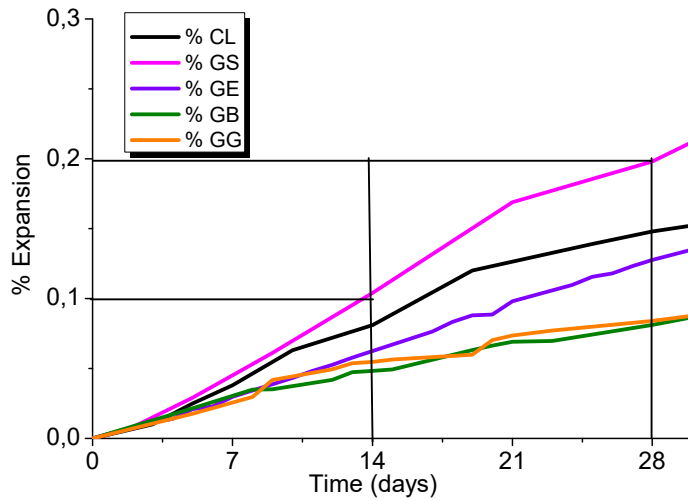


FIGURE 3: Evolution of the expansion of the mortars manufactured with different aggregates at 28 days

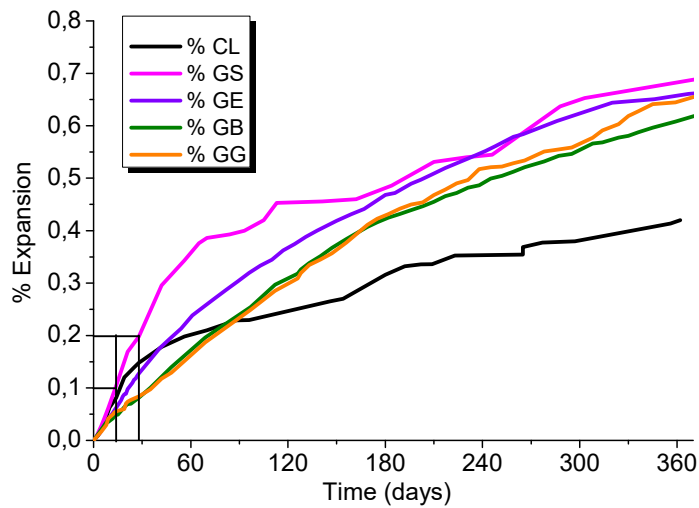


FIGURE 4: Evolution of the expansion of the mortars manufactured with different aggregates at 365 days

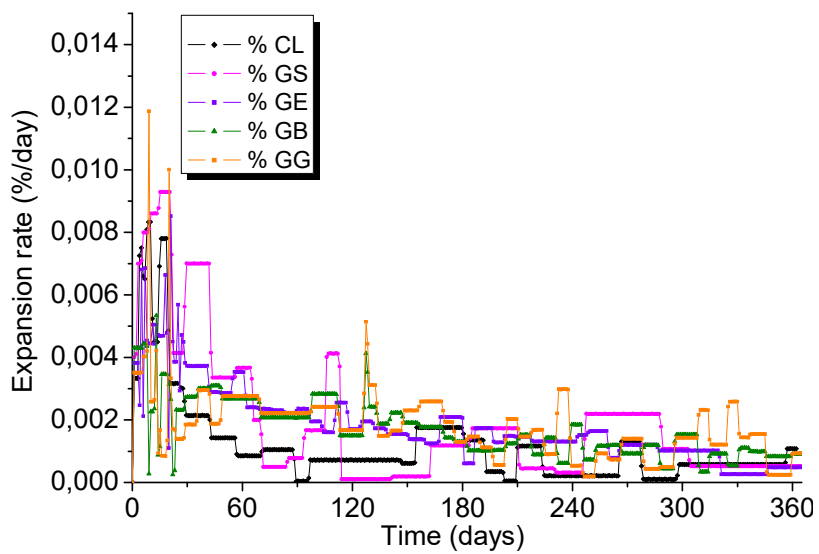


FIGURE 5: Evolution of the expansion ratio.